

Structures and Magnetic Properties of Two Analogous Dy₆ Wheels with Electron-Donation and -Withdrawal Effects

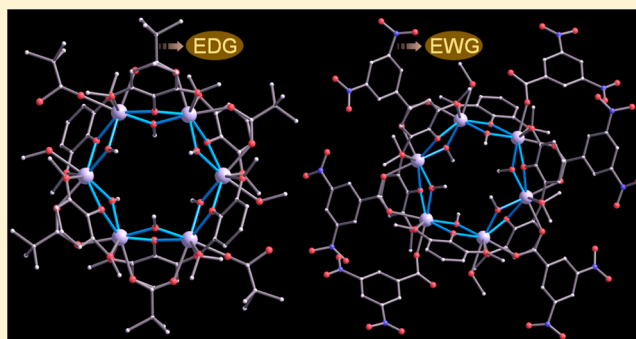
Biplab Joarder,[†] Soumya Mukherjee,[†] Shufang Xue,[‡] Jinkui Tang,^{*,‡} and Sujit K. Ghosh^{*,†}

[†]Indian Institute of Science Education and Research (IISER), Dr. Homi Bhabha Road, Pashan, Pune-411008, India

[‡]State Key Laboratory of Rare Earth Resource Utilization, Changchun, Institute of Applied Chemistry, Chinese Academy of Sciences, Changchun, 130022, China

Supporting Information

ABSTRACT: Two new hexanuclear symmetric dysprosium wheels, namely, [Dy₆(L₁)₆(L')₆(OCH₃)₆(2CH₃OH)] and [Dy₆(L₂)₆(L')₆(OCH₃)₆(2CH₃OH)] (L₁H = pivalic acid and L₂H = 3,5-dinitrobenzoic acid, L'H = 2,6-dimethoxyphenol) were isolated employing a mixed-ligand strategy. The strategic introduction of two different auxiliary groups with diverse steric effects and electrostatic actions affect the magnetic coupling and local anisotropy of Dy^{III} ion, therefore exhibiting dissimilar magnetic behaviors.



INTRODUCTION

The seminal discovery of single molecule magnet (SMM) behavior^{1,2} in dodecanuclear mixed-valent manganese (III/IV) cluster³ triggered the persistent drive right through the past decade, to develop novel molecular magnets aimed to miniaturize devices in the nanoregime involving high-density information storage, quantum computing, and molecule spintronics.⁴ SMMs are molecular species typically characterized by the slow relaxation of the magnetization due to the unique combination of both high-spin (*S*) ground state and uniaxial (negative) magnetic anisotropy (*D*), leading to an anisotropy energy barrier (*U*) for the concomitant reversal of magnetization vector $S^2|D|$.⁵ After the initial extensive study on polynuclear 3d metal aggregates, especially large manganese complexes, was carried out as a prime focus by chemists, physicists, and material scientists,⁶ recent years have particularly seen a flurry of interesting results out of lanthanide-based SMMs,⁷ including the achievement of maximum relaxation energy barriers⁸ for multinuclear clusters and the highest blocking temperature.⁹ This promising strategy to design novel homometallic lanthanide-based SMMs solely benefit from the significant magnetic anisotropy of lanthanide ions such as Dy^{III} owing to their inherently large, unquenched orbital angular momentum.¹⁰ Since the SMM behavior has been established to be directed by the crucial interplay of the ligand field effect, coordination geometry, and the strength of the magnetic interactions between the neighboring lanthanide sites, the design of coordination chemistry assemblies represents a key avenue for accessing tailor-made functional SMMs.¹¹

Whereas the energy barriers (giving rise to magnetic bistability and slow magnetization relaxation) have been

following a trend of steady escalation with diverse-natured novel molecular clusters, a more systematic approach is essentially required to elucidate the origin of slow relaxation as well as target rational methods of synthesizing better SMMs. This led to the mixed-ligand based strategy¹² to synthesize two analogous dysprosium-based SMMs, differing only in the nature of the respective coordinated carboxylic acid ligands. As a point of reference, very recently the effects of electron-withdrawing substituents on the energy barrier-enhancement for five novel Dy₂ SMMs has been shown as the first report of a direct correlation between relaxation barriers and electron-withdrawing groups on terminal ligands while retaining the geometry of the lanthanide ions intact.¹³

Herein, we report two dysprosium-based symmetric hexanuclear wheel compounds (Dy₆), namely, [Dy₆(L₁)₆(L')₆(OCH₃)₆(2CH₃OH)] (**1**) and [Dy₆(L₂)₆(L')₆(OCH₃)₆(2CH₃OH)] (**2**) (L₁H = pivalic acid, L₂H = 3,5-dinitrobenzoic acid, and L'H = 2,6-dimethoxyphenol) by the designed variation principle of the participating carboxylic acid ligands (Figure 1), aimed to study the differential effects of the opposite-natured ligands on the SMM property for these two analogous molecular magnets.

The electron-rich pivalic acid (L₁H) ligands are expected to make the central wheel electron-rich owing to +I effects of the three methyl groups; as a parallel event, the highly electron-withdrawing -R effect of nitro groups in the analogous ligand 3,5-dinitrobenzoic acid leaves the other Dy₆ wheel somewhat electron-deficient. This differential nature of electron-density of

Received: April 14, 2014

Published: July 7, 2014

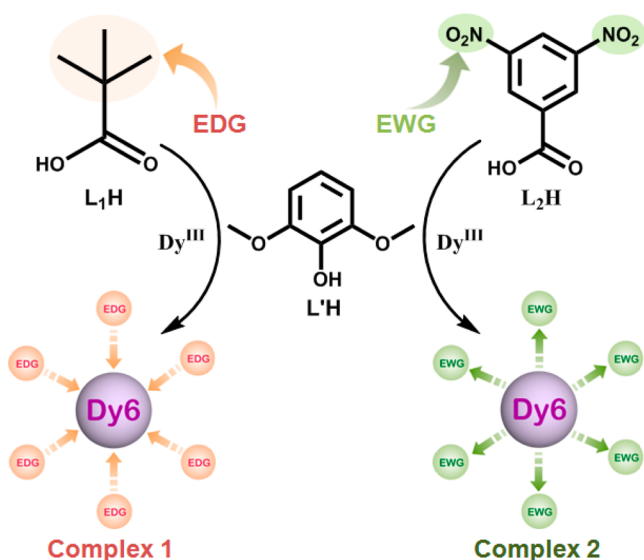


Figure 1. Mixed-ligand-based strategy to synthesize complexes **1** and **2**.

six of the terminal bridging ligands is expected to affect the exchange-coupling and ring current phenomena operative in compounds **1** and **2** (Figure 2), which led to the strategic design and synthesis of these symmetric Ln_6 -wheel complexes and consequent investigation of the magnetic properties for these.

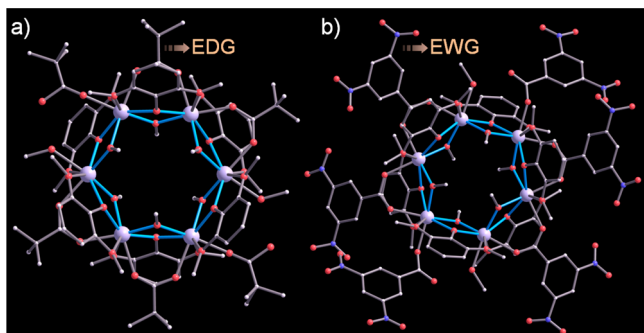


Figure 2. Molecular structures of complexes **1** and **2**, highlighting the difference in terminal (a) electron-donating group (EDG) and (b) electron-withdrawing group (EWG).

EXPERIMENTAL SECTION

Materials and Measurements. All the reagents and solvents were commercially available and used without further purification. X-ray powder pattern was recorded on Bruker D8 Advanced X-ray diffractometer at room temperature using $\text{Cu K}\alpha$ radiation ($\lambda = 1.5406 \text{ \AA}$). Fourier transform infrared (FT-IR) spectra were measured on NICOLET 6700 FT-IR Spectrophotometer using KBr pellets. Thermogravimetric analyses were obtained in the temperature range of 30–800 °C on PerkinElmer STA 6000 analyzer under a N_2 atmosphere at a heating rate of 10 °C min^{-1} . Magnetic measurements were performed in the temperature range of 2–300 K using Quantum Design MPMS-XL SQUID and 1.9–5.0 K using SQUID-VSM magnetometers, respectively. The diamagnetic corrections for the compounds were estimated using Pascal's constants, and magnetic data were corrected for diamagnetic contributions of the sample holder.

Synthesis of $[\text{Dy}_6(\text{L}_1)_6(\text{L}')_6(\text{OCH}_3)_6(2\text{CH}_3\text{OH})]$ (1**).** A methanolic solution of L_1H (51.06 mg, 0.5 mmol in 5 mL) was deprotonated with

triethylamine (139.5 μL , 1 mmol), to which solid $\text{L}'\text{H}$ (77.08 mg, 0.5 mmol) was slowly added while sonicating the reaction mixture. The solution was diluted with the addition of a binary solvent mixture of MeOH/MeCN (9 mL/10 mL respectively), followed by the addition of 1 mL of methanolic solution of dysprosium nitrate hydrate (136.98 mg, 0.3 mmol). The mixture was kept in undisturbed conditions at room temperature, as colorless crystals of compound **1** suitable for single-crystal X-ray analysis was obtained after slow evaporation of the binary solvent mixture of MeOH/MeCN for 3 d. ~58% yield. IR (KBr, cm^{-1}): 3666 (s), 3433(w), 2963(s), 1587(m), 1494(w), 1367(m), 1236(s), 1164(w), 1101(vs), 1029(s), 894(s), 793(s), 716 (m), 598(w), 553(m). Anal. Calcd (found) for $\text{C}_{86}\text{H}_{134}\text{O}_{38}\text{Dy}_6$: C, 37.55 (37.51); H, 4.91 (4.97)%.

Synthesis of $[\text{Dy}_6(\text{L}_2)_6(\text{L}')_6(\text{OCH}_3)_6(2\text{CH}_3\text{OH})]$ (2**).** Solid dysprosium(III) nitrate hydrate (45.7 mg, 0.1 mmol) was added to a well-sonicated mixture of MeOH/EtOAc (3:7) solution of L_2H (0.1 mM) and $\text{L}'\text{H}$ (0.2 mM), neutralized by triethylamine (41.5 μL , 0.3 mmol). Intense yellow crystals of compound **2** suitable for single-crystal X-ray analysis was obtained after only 2 h of slow evaporation in undisturbed condition. ~52% yield. IR (KBr, cm^{-1}): 3665 (m), 3099(m), 2944(w), 2841(vw), 1635(m), 1541(vw), 1463(w), 1295(m), 1242(m), 1163(m), 1069(vs), 1018(m), 919(m), 850(m), 799(s), 767(vw), 721(s), 652(vw), 545.22(m), 440(w). Anal. Calcd (found) for $\text{C}_{98}\text{H}_{104}\text{N}_{12}\text{O}_{56}\text{Dy}_6$: C, 35.44 (35.38); H, 3.16 (3.24); N, 5.06 (5.05)%.

X-ray Structural Studies. Single-crystal X-ray data of **1** and **2** were collected at 200 K on a Bruker KAPPA APEX II CCD Duo diffractometer (operated at 1500 W power: 50 kV, 30 mA) using graphite-monochromated Mo $\text{K}\alpha$ radiation ($\lambda = 0.71073 \text{ \AA}$). Crystal was mounted on nylon CryoLoops (Hampton Research) with Paratone-N (Hampton Research). The data integration and reduction were processed with SAINT¹⁴ software. A multiscan absorption correction was applied to the collected reflections. The structure was solved by the direct method using SHELXTL¹⁵ and was refined on F^2 by full-matrix least-squares technique using the SHELXL-97¹⁶ program package within the WINGX¹⁷ program. All non-hydrogen atoms were refined anisotropically. All hydrogen atoms were located in successive difference Fourier maps and were treated as riding atoms using SHELXL default parameters. The structures were examined using the Adsym subroutine of PLATON¹⁸ to ensure that no additional symmetry could be applied to the models. Crystal data and structure refinement details for complexes **1** and **2** are summarized in Table 1.

Magnetic Measurement (Experimental) Details. Magnetic measurements were performed in the temperature range of 2–300 K using Quantum Design MPMS-XL SQUID and 1.9–5.0 K using SQUID-VSM magnetometers, respectively. The diamagnetic corrections for the compounds were estimated using Pascal's constants, and magnetic data were corrected for diamagnetic contributions of the sample holder.

RESULTS AND DISCUSSION

Compounds **1** and **2** were prepared at room temperature by slow evaporation of the respective reaction mixtures. Single-crystal X-ray analysis reveals that both compounds were crystallized in triclinic space group $P\bar{1}$ with $Z = 2$ and $Z = 1$, respectively. The molecular structure of compound **1** (with partial labeling), presenting the central wheel-shaped core, is shown in Figure 3, while the similar one for compound **2** is shown in Figure 4. TGA data for these compounds (Supporting Information, Figures S5 and S6) show significant thermal stability up to nearly 250 °C with no weight loss, corresponding to the absence of any guest molecule in both of the air-dried phases. Compound **1** crystallized in two crystallographically unique, but structurally similar Dy_6 units; hence, only one is considered in the ensuing discussion. For compound **1**, the asymmetric unit of the hexanuclear cluster contains the assembly of three dysprosium ions, namely, Dy1, Dy2, and Dy3. Both the pairs of Dy1, Dy2 and Dy2, Dy3 are connected

Table 1. Crystal data and structure refinement for 1 and 2

identification code	compound 1	compound 2
empirical formula	C ₈₆ H ₁₃₄ Dy ₆ O ₃₈	C ₉₈ H ₉₈ Dy ₆ N ₁₂ O ₆₂
formula weight	2750.93	3410.88
temperature/K	200(2)	200(2)
wavelength/Å	0.710 73	0.710 73
crystal system	triclinic	triclinic
space group	P $\bar{1}$	P $\bar{1}$
a/Å	16.873(2)	11.0686(18)
b/Å	17.570(2)	17.344(3)
c/Å	22.008(3)	19.330(3)
α /deg	99.709(3)	113.975(3)
β /deg	105.197(2)	100.420(3)
γ /deg	112.518(2)	100.367(3)
V/Å ³	5545.0(13)	3199.3(9)
Z	2	1
D/mg m ⁻³	1.648	1.77
μ /mm ⁻¹	4.065	3.558
F(000)	2700	1662
θ range (deg)	1.81 to 28.46	1.20 to 28.49
reflections collected	88 813	50 463
independent reflections	27 841	15 631
completeness	99.30%	96.50%
data/restraints/parameters	27841/12/1171	15631/16/777
GOF	1.308	1.043
R ₁ , wR ₂ [<i>I</i> > 2 σ (<i>I</i>)]	0.0439, 0.1674	0.0807, 0.2195
R ₁ , wR ₂ (all data)	0.0543, 0.1760	0.1954, 0.2963

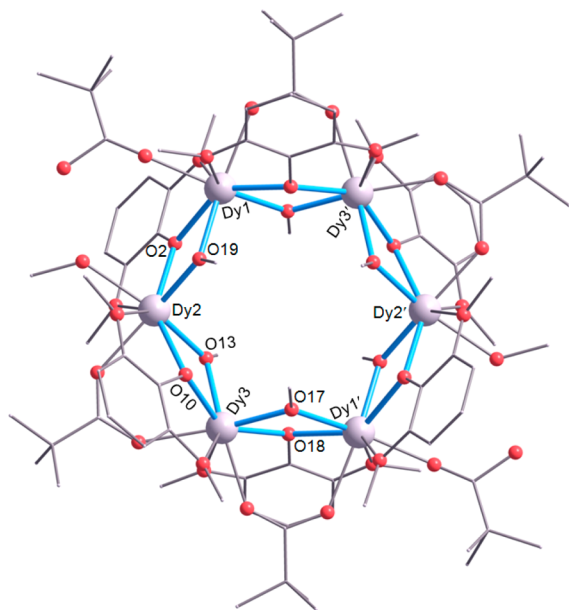


Figure 3. Partially labeled crystal structure of complex 1, presenting the central core of the molecular magnet. H atoms are omitted for clarity.

via a μ_2 -alkoxy (methoxy) bridge, and the ligand L' bridging over each pair of the two metal centers exactly in the similar way. The proximate pair of Dy1 and Dy2 is bridged by O19-methoxy, and the analogous pair of Dy2 and Dy3 is bridged by O13-methoxy bridge, both in μ_2 -fashion.

While O1, O3 and O11, O9 from the methoxy groups of two L' ligands coordinate to the Dy-centers individually, the deprotonated hydroxyl oxygens for these two ligands, namely, O2 and O10, coordinate to the metal centers in μ_2 -bridging

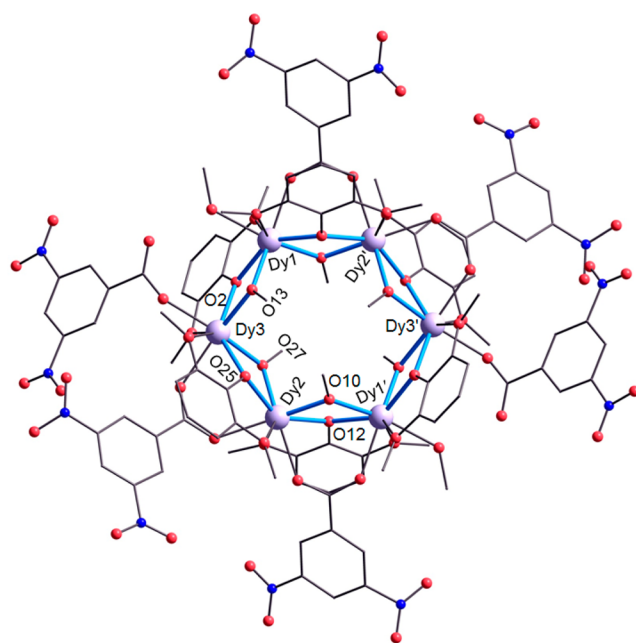


Figure 4. Partially labeled crystal structure of complex 2, presenting the central core of the molecular magnet. H atoms are omitted for clarity.

fashion. Each of the terminal Dy3 and Dy1 centers are also coordinated by the deprotonated pivalate ligands (L₁), while the charge balance on the Dy1 center occurs because of the simultaneous η^2 -mode binding of the ligand L' (via O12 and O18) (Supporting Information, Figure S8). There is one distinct –OCH₃ coordination to the central Dy₂ center, arising out of the reaction mixture solvent MeOH employed herein. The intermetallic distances of the Dy-centers in the symmetric wheel are nearly similar: Dy1–Dy2 = 3.736 Å and Dy2–Dy3 = 3.732 Å, respectively. The Dy–O–Dy bond angles are 105.72° (Dy1–O2–Dy2), 111.62° (Dy1–O19–Dy2) for the vicinal pair of Dy1 and Dy2, whereas the analogous Dy–O–Dy bond angles are 105.44° (Dy2–O10–Dy3) and 111.82° (Dy2–O13–Dy3) for the neighboring couple of Dy2 and Dy3. All six Dy(III) centers adopt dodecahedral coordination environments in the homometallic wheel (Supporting Information, Figure S2). There is significant intramolecular H-bonding interaction interplaying between O5 of pivalate and O16 from the methoxy group coordinated to the central Dy₂ center.

For compound 2, similar to the analogous compound 1, the asymmetric unit of this hexanuclear cluster also comprises of the assemblage of three Dy^{III} ions, precisely, Dy1, Dy2, and Dy3, wherein the pairs of Dy1, Dy2 and Dy2, Dy3 are linked via a μ_2 -alkoxy (methoxy) bridge and the ligand L' spanning over each of the pair of the two metal centers just in a manner akin to compound 1. The contiguous pair of Dy1 and Dy2 are μ_2 -bridged by O12 methoxy, and the similar pair of Dy2 and Dy3 are similarly bridged by O27 methoxy group. While O9, O11 and O24, O26 of the two L' ligands coordinate to the Dy centers individually, the deprotonated hydroxyl oxygens for these two ligands, namely, O10 and O25, coordinate to the metal centers in μ_2 -bridging mode. Each of the adjacent Dy1 and Dy3 centers are coordinated by the deprotonated 3,5-dinitrobenzoate ligands (L₂) in μ_2 -bridging fashion (via O5 and O21), while the charge balance on the Dy2 center ensues from the direct coordination of the ligand L₂ (through O14) (Supporting Information, Figure S8). There is one distinct

–OCH₃ coordination to the terminal Dy₁ center via O28, owing to the involved reaction mixture solvent MeOH. The intermetallic distances of the Dy centers in the symmetric wheel are nearly similar: Dy₁–Dy₂ = 3.780 Å and Dy₂–Dy₃ = 3.719 Å. The Dy–O–Dy bond angles are 114.54° (Dy₁–O12–Dy₂) and 109.63° (Dy₁–O10–Dy₂) for the proximal pair of Dy₁ and Dy₂, whereas the corresponding bond angles are 105.18° (Dy₂–O25–Dy₃) and 111.90° (Dy₂–O27–Dy₃) for the adjoining couple of Dy₂ and Dy₃. Each of the Dy(III) centers assumes dodecahedral coordination environment in the central core (Supporting Information, Figure S2). It is noteworthy that there are 2-fold intramolecular H-bonding interactions existent between two separate pairs. One is between O16 and O30 from two distinct nitro groups of two different L₂ ligands both connected to Dy₂ center. The other one is between O15 of deprotonated L₂ and O28 of methoxy group coordinated to the terminal Dy₁ center.

Direct current (dc) magnetic susceptibilities for compounds **1** and **2** were measured in an applied magnetic field of 1000 Oe between 300 and 2 K. At room temperature, the $\chi_M T$ values are 82.45 and 80.32 cm³ K mol⁻¹ for **1** and **2**, respectively (Figure 5), which are in agreement with the expected value of 85.02

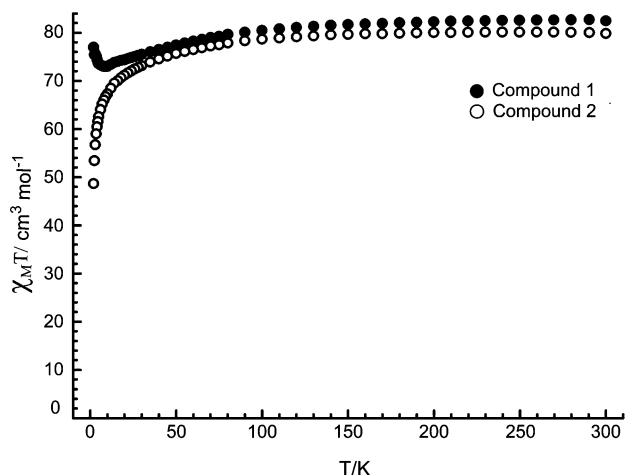


Figure 5. Temperature dependences of $\chi_M T$ on T for **1** and **2** under 1000 Oe field, χ_M being molar magnetic susceptibility.

cm³ K mol⁻¹ for six uncoupled Dy^{III} ions ($C = 14.18$ cm³ K mol⁻¹). Upon cooling, the $\chi_M T$ values for both compounds gradually decrease from 300 to 50 K due to the depopulation of the Stark sublevels and/or significant magnetic anisotropy present in Dy systems. However, upon further decrease of temperature (below 50 K), these compounds exhibit different thermal behavior and quite significant difference from other Dy₆ wheels with net toroidal magnetic moment.¹⁹

For compound **1**, after reaching a minimum of 72.98 cm³ K mol⁻¹ at 9 K, the $\chi_M T$ product starts to increase up to the maximum of 76.97 cm³ K mol⁻¹ at 2 K, indicative of the presence of intramolecular weak ferromagnetic interactions between Dy^{III} spin carriers as observed in other dysprosium systems,²⁰ while the $\chi_M T$ of compound **2** further decreases rapidly to reach 48.66 cm³ K mol⁻¹ at 2 K. This thermal evolution may be ascribed to very weak antiferromagnetic magnetic interactions between Dy^{III} ions. These behaviors are consistent with the field dependence of the magnetization at 2 K. Magnetization (M) data for **1** and **2** were collected in the 0–70 kOe field range below 5 K. The field dependence of M

shows that M increases smoothly with increasing applied dc field without saturation even at 7 T, which is ascribed to the anisotropy and the crystal-field effect.²¹ Both the nonsaturated magnetization even at 7 T (Figure 6) and the nonsuperimposed M versus H/T plot (Figure 7) indicates the presence of significant magnetic anisotropy and/or low-lying excited states.

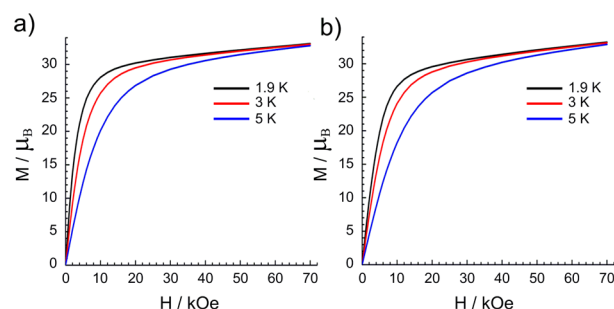


Figure 6. Plots of M vs H at the indicated temperatures (a) for **1** and (b) for **2**.

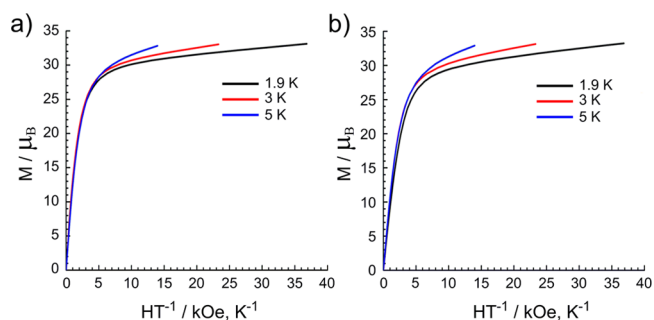


Figure 7. Plots of the reduced magnetization M vs H/T in the field range of 0–70 kOe and temperature range of 1.9–5.0 K for **1** (a) and **2** (b).

The alternating current (ac) susceptibilities measurements were performed under zero static field and a 3.0 Oe ac field oscillating at various frequencies from 1 to 1500 Hz. Both frequency- and temperature-dependent ac susceptibilities for **1** and **2** reveal the presence of slow relaxation of the magnetization, typical of SMM behavior (Figures 8 and 9).

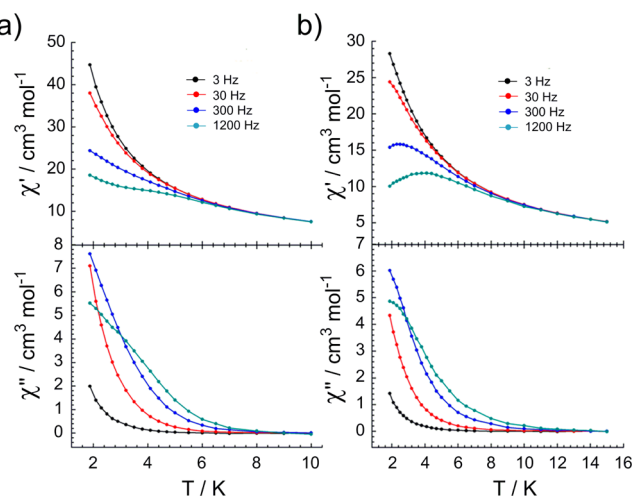


Figure 8. Temperature dependence of ac susceptibilities under zero field at indicated frequencies (a) for **1** and (b) for **2**.

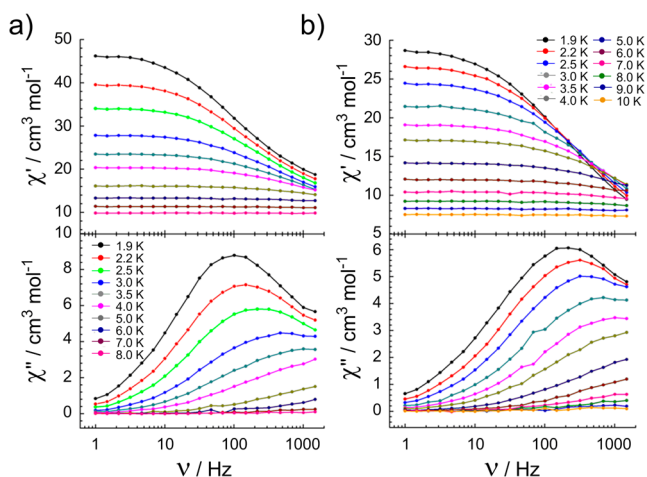


Figure 9. Frequency dependence of ac susceptibilities under zero field below 10 K (a) for **1** and (b) for **2**.

The energy barrier and characteristic relaxation time can be obtained for **1** and **2** by fitting the magnetization time (τ) extracted from the frequency-dependent ac susceptibility with the Arrhenius law $\tau = \tau_0 \exp(U_{\text{eff}}/k_{\text{B}}T)$, giving $U_{\text{eff}} = 12.2(1)$ and $11.5(1)$ K, and pre-exponential factors of $\tau_0 = 5.0(1) \times 10^{-6}$ and $5.1(1) \times 10^{-6}$, respectively (Figure 10). These

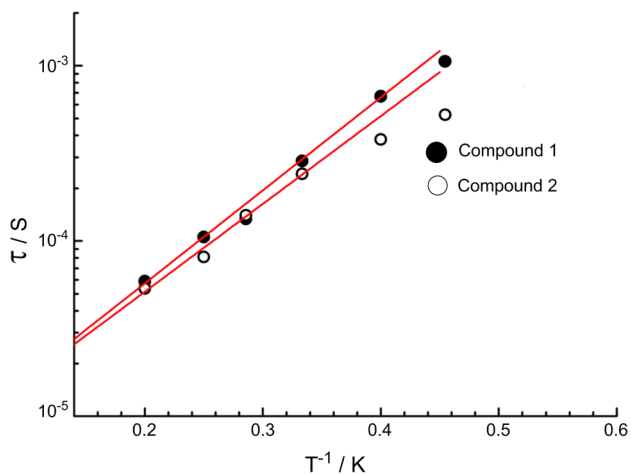


Figure 10. Magnetization relaxation time τ vs T^{-1} plots for **1** and **2**. The solid line is fitted with the Arrhenius law.

dynamic magnetic behaviors are quite similar to small relaxation barriers and large pre-exponential factors due to the fast relaxation rates. The slight difference is the frequency-dependent maximum, which is expected when the frequency equals the rate of the relaxation process taking place at a temperature somewhat lower in case of **2**, corresponding to the reported lower U_{eff} for **2**.

Close inspection of the geometry of the Dy^{III} ions in **1** and **2**, reflecting from the determination by SHAPE 2.0 software, indicates that dysprosium(III) centers are ascribed to the distorted dodecahedron (D_{2d}) (Supporting Information, Table S3). The distorted dodecahedral geometry of Dy^{III} center may induce a larger angle between the easy axis and the idealized tetragonal axis of the dodecahedron, therefore resulting in greater importance of transverse anisotropy terms, thus largely prone to quantum tunneling.²²

To further probe the structural–magnetic relationship, some crucial parameters of the structures are listed in Supporting Information, Table S4. It is noteworthy that both compounds have similar Dy–O–Dy angles, but compound **2** displays the shorter Dy–O bonds, which are induced by the electrostatic action and bulky steric effect from the terminal counterions in **2**, thus directing toward influencing the dynamical behavior. Indeed, the electron-withdrawing groups (NO_2) in **2** lead to an increase in the Dy–O_{terminal} bond lengths and a relatively stronger chemical bonding between Dy–O linkages, which influence the relaxation rate in the low-temperature regime compared to **1**. It is worth mentioning that the exchange coupling usually predominates the magnetic dynamics, which is confirmed by an example of such a paradigm shift provided by a series of Dy_2 compounds.²³ It is evident that minor changes occurring in the structure, such as the ones observed for Dy_4K_2 and Dy_5 compounds,²⁴ could produce dramatic changes in magnetic coupling and single-ion anisotropy, thus influencing the magnetic dynamics. However, it is indeed quite surprising that there are no such big differences in the dynamic behavior for compounds **1** and **2**, in spite of their quite different static magnetic behaviors shown in Figure 5.

CONCLUSION

Herein we report two analogous hexanuclear dysprosium wheels assembled by adopting a mixed-ligand strategy based on two precisely divergent natured ligands with two types of auxiliary groups. Magnetic analysis reveals that both compounds show similar dynamic magnetic behaviors. However, the differential nature of electron-density of six of the terminal bridging ligands affects the exchange-coupling operative in these compounds, and thus their static magnetic behaviors are quite different. Further studies into the static and dynamic magnetic differences induced by the introduction of different auxiliary groups with distinct steric effect and electrostatic actions are under way in our group.

ASSOCIATED CONTENT

Supporting Information

Coordination polyhedra, PXRD patterns, TGA data, FTIR spectra, connection modes, crystallographic data tables, and magnetism data tables. This material is available free of charge via the Internet at <http://pubs.acs.org>.

AUTHOR INFORMATION

Corresponding Authors

*E-mail: sghosh@iiserpune.ac.in. Fax: +91 20 2590 8186. (S.K.G.)

*E-mail: tang@ciac.jl.cn. (J.T.)

Author Contributions

B.J. and S.M. have contributed equally.

Notes

The authors declare no competing financial interest.

ACKNOWLEDGMENTS

B.J. is thankful to CSIR for research fellowship. We are grateful to IISER Pune for research facilities. DAE (Project No. 2011/20/37C/06/BRNS) and DST (Project No. GAP/DST/CHE-12-0083) are acknowledged for the financial support.

REFERENCES

- (1) (a) Zaleski, C. M.; Depperman, E. C.; Kampf, J. W.; Kirk, M. L.; Pecoraro, V. L. *Angew. Chem., Int. Ed.* **2004**, *43*, 3912–3914. (b) Gatteschi, D.; Sessoli, R. Villain, J. *Molecular Nanomagnets*; Oxford University Press: Oxford, U.K., 2006. (c) Lin, P.-H.; Burchell, T. J.; Clérac, R.; Murugesu, M. *Angew. Chem., Int. Ed.* **2008**, *47*, 8848–8851. (d) Costes, J. P.; Shova, S.; Wernsdorfer, W. *Dalton Trans.* **2008**, 1843–1849. (e) Chibotaru, L.; Ungur, L.; Soncini, A. *Angew. Chem., Int. Ed.* **2008**, *47*, 4126–4129. (f) Gamer, M.; Lan, Y.; Roesky, P. W.; Powell, A. K.; Clerac, R. *Inorg. Chem.* **2008**, *47*, 6581–6583. (g) Zheng, Y. Z.; Lan, Y.; Anson, C. E.; Powell, A. K. *Inorg. Chem.* **2009**, *47*, 10813–10815. (h) Burrow, C. E.; Burchell, T. J.; Lin, P. H.; Habib, F.; Wernsdorfer, W.; Clerac, R.; Murugesu, M. *Inorg. Chem.* **2009**, *48*, 8051–8053. (i) Xu, G. F.; Wang, Q. L.; Gamez, P.; Ma, Y.; Clerac, R.; Tang, J.; Yan, S. P.; Cheng, P.; Liao, D. Z. *Chem. Commun.* **2010**, *46*, 1506–1508.
- (2) (a) Ishikawa, N.; Sugita, M.; Ishikawa, T.; Koshihara, S.; Kaizu, Y. *J. Am. Chem. Soc.* **2003**, *125*, 8694–8695. (b) Luzon, J.; Bernot, K.; Hewitt, I. J.; Anson, C. E.; Powell, A. K.; Sessoli, R. *Phys. Rev. Lett.* **2008**, *100*, 247205–1–247205–4. (c) Lin, P. H.; Burchell, T. J.; Ungur, L.; Chibotaru, L. F.; Wernsdorfer, W.; Murugesu, M. *Angew. Chem., Int. Ed.* **2009**, *48*, 9489–9492. (d) AlDamen, M. A.; Clemente-Juan, J. M.; Coronado, E.; Marti-Gastaldo, C.; Gaita-Ariño, A. *J. Am. Chem. Soc.* **2008**, *130*, 8874–8875. (e) Cardona-Serra, S.; Clemente-Juan, J. M.; Coronado, E.; Gaita-Ariño, A.; Camón, A.; Evangelisti, M.; Luis, F.; Martínez Pérez, M. J.; Sesé, J. J. *J. Am. Chem. Soc.* **2012**, *134*, 14982–14990. (f) Joarder, B.; Chaudhari, A. K.; Rogez, G.; Ghosh, S. K. *Dalton Trans.* **2012**, *41*, 7695–7699.
- (3) (a) Caneschi, A.; Gatteschi, D.; Sessoli, R.; Barra, A. L.; Brunel, L. C.; Guillot, M. *J. Am. Chem. Soc.* **1991**, *113*, 5873–5874. (b) Sessoli, R.; Hui, L.; Schake, A. R.; Wang, S.; Vincent, J. B.; Folting, K.; Gatteschi, D.; Christou, G. *J. Am. Chem. Soc.* **1993**, *115*, 1804–1816. (c) Sessoli, R.; Gatteschi, D.; Caneschi, A.; Novak, M. A. *Nature* **1993**, *365*, 141–143. (d) Gatteschi, D.; Caneschi, A.; Pardi, L.; Sessoli, R. *Science* **1994**, *265*, 1054–1058.
- (4) (a) Leuenberger, M. N.; Loss, D. *Nature* **2001**, *410*, 789–793. (b) Coronado, E.; Day, P. *Chem. Rev.* **2004**, *104*, 5419–5448. (c) Ardavan, A.; Rival, O.; Morton, J. J. L.; Blundell, S. J.; Tyryshkin, A. M.; Timco, G. A.; Winpenny, R. E. P. *Phys. Rev. Lett.* **2007**, *98*, 057201–1–057201–4. (d) Bouchiat, V.; Wernsdorfer, W.; Balestro, F. *Nature* **2008**, *453*, 633–637. (e) Bogani, L.; Wernsdorfer, W. *Nat. Mater.* **2008**, *7*, 179–186. (f) Mannini, M.; Pineider, F.; Danieli, C.; Totti, F.; Sorace, L.; Sainctavit, P.; Arrio, M. A.; Otero, E.; Joly, L.; Cezar, J. C.; Cornia, A.; Sessoli, R. *Nature* **2010**, *468*, 417–421. (g) Urdampilleta, M.; Nguyen, N. V.; Cleuziou, J. P.; Klyatskaya, S.; Ruben, M.; Wernsdorfer, W. *Int. J. Mol. Sci.* **2011**, *12*, 6656–6667. (h) Rinehart, J. D.; Fang, M.; Evans, W. J.; Long, J. R. *Nat. Chem.* **2011**, *3*, 538–542. (i) Katoh, K.; Isshiki, H.; Komeda, T.; Yamashita, M. *Chem.—Asian J.* **2012**, *7*, 1154–1169.
- (5) (a) Christou, G.; Gatteschi, D.; Hendrickson, D. N.; Sessoli, R. *MRS Bull.* **2000**, *25*, 66–71. (b) Chaudhari, A. K.; Joarder, B.; Riviere, E.; Rogez, G.; Ghosh, S. K. *Inorg. Chem.* **2012**, *51*, 9159–9161. (c) Luzon, J.; Sessoli, R. *Dalton Trans.* **2012**, *41*, 13556–13567. (d) Zhang, P.; Guo, Y. N.; Tang, J. *Coord. Chem. Rev.* **2013**, *257*, 1728–1763. (e) Woodruff, D. N.; Winpenny, R. E. P.; Layfield, R. A. *Chem. Rev.* **2013**, *113*, 5110–5148. (f) Habib, F.; Murugesu, M. *Chem. Soc. Rev.* **2013**, *42*, 3278–3288.
- (6) (a) Boskovic, C.; Brechin, E. K.; Streib, W. E.; Folting, K.; Bollinger, J. C.; Hendrickson, D. N.; Christou, G. *J. Am. Chem. Soc.* **2002**, *124*, 3725–3736. (b) Brechin, E. K.; Boskovic, C.; Wernsdorfer, W.; Yoo, J.; Yamaguchi, A.; Sañudo, E. C.; Concolino, T. R.; Rheingold, A. L.; Ishimoto, H.; Hendrickson, D. N.; Christou, G. *J. Am. Chem. Soc.* **2002**, *124*, 9710–9711. (c) King, P.; Wernsdorfer, W.; Abboud, K. A.; Christou, G. *Inorg. Chem.* **2004**, *43*, 7315–7323. (d) Zheng, Y.-Z.; Xue, W.; Zhang, W.-X.; Tong, M.-L.; Chen, X.-M. *Inorg. Chem.* **2007**, *46*, 6437–6443. (e) Manoli, M.; Johnstone, R. D. L.; Parsons, S.; Murrie, M.; Affronte, M.; Evangelisti, M.; Brechin, E. K. *Angew. Chem., Int. Ed.* **2007**, *46*, 4456–4460. (f) Feng, P. L.; Stephenson, C. J.; Amjad, A.; Ogawa, G.; Barco, E. d.; Hendrickson, D. N. *Inorg. Chem.* **2010**, *49*, 1304–1306. (g) Stamatatos, T. C.; -Albiol, D. F.; Wernsdorfer, W.; Abbouda, K. A.; Christou, G. *Chem. Commun.* **2011**, *47*, 274–276. (h) Nayak, S.; Evangelisti, M.; Powell, A. K.; Reedijk, J. *Chem.—Eur. J.* **2010**, *16*, 12865–12872. (i) Kotzabasaki, V.; Inglis, R.; Siczek, M.; Lis, T.; Brechin, E. K.; Milios, C. J. *Dalton Trans.* **2011**, *40*, 1693–1699. (j) Yang, C.-L.; Yang, S.-F.; Hung, S.-P.; Lee, G.-H.; Wurd, C.-S.; Tsai, H.-L. *Polyhedron* **2011**, *30*, 2969–2977. (k) Costa, J. S.; Barrios, L. A.; Craig, G. A.; Teat, S. J.; Luis, F.; Roubeau, O.; Evangelisti, M.; Camón, A.; Aromí, G. *Chem. Commun.* **2012**, *48*, 1413–1415. (l) Charalambous, M.; Moushi, E. E.; Papatriantafyllopoulou, C.; Wernsdorfer, W.; Nastopoulos, V.; Christou, G.; Tasiopoulos, A. J. *Chem. Commun.* **2012**, *48*, 5410–5412. (m) Chakraborty, A.; Ghosh, B. K.; -Arino, J. R.; Ribas, J.; Maji, T. K. *Inorg. Chem.* **2012**, *51*, 6440–6442.
- (7) (a) Chakov, N. E.; Lee, S.-C.; Harter, A. G.; Kuhns, P. L.; Reyes, A. P.; Hill, S. O.; Dalal, N. S.; Wernsdorfer, W.; Abboud, K. A.; Christou, G. *J. Am. Chem. Soc.* **2006**, *128*, 6975–6989. (b) Ishikawa, N.; Mizuno, Y.; Takamatsu, S.; Ishikawa, T.; Koshihara, S.-y. *Inorg. Chem.* **2008**, *47*, 10217–10219. (c) Milios, C. J.; Vinslava, A.; Wernsdorfer, W.; Moggach, S.; Parsons, S.; Perlepes, S. P.; Christou, G.; Brechin, E. K. *J. Am. Chem. Soc.* **2007**, *129*, 2754–2755. (d) Yoshihara, D.; Karasawa, S.; Koga, N. *J. Am. Chem. Soc.* **2008**, *130*, 10460–10461. (e) Magnani, N.; Colineau, E.; Eloirdi, R.; Griveau, J.-C.; Caciuffo, R.; Cornet, S. M.; May, I.; Sharrad, C. A.; Collison, D.; Winpenny, R. E. P. *Phys. Rev. Lett.* **2010**, *104*, 197202–1–197202–4. (f) Guo, Y.-N.; Xu, G.-F.; Gamez, P.; Zhao, L.; Lin, S.-Y.; Deng, R.; Tang, J.; Zhang, H.-J. *J. Am. Chem. Soc.* **2010**, *132*, 8538–8539. (g) Hewitt, I. J.; Tang, J.; Madhu, N. T.; Anson, C. E.; Lan, Y.; Luzon, J.; Etienne, M.; Sessoli, R.; Powell, A. K. *Angew. Chem., Int. Ed.* **2010**, *49*, 6352–6356. (h) Jiang, S.-D.; Wang, B.-W.; Sun, H.-L.; Wang, Z.-M.; Gao, S. *J. Am. Chem. Soc.* **2011**, *133*, 4730–4733. (i) Watanabe, A.; Yamashita, A.; Nakano, M.; Yamamura, T.; Kajiwara, T. *Chem.—Eur. J.* **2011**, *17*, 7428–7432. (j) Gonidec, M.; Luis, F.; Vilchez, À.; Esquena, J.; Amabilino, D. B.; Veciana, J. *Angew. Chem., Int. Ed.* **2010**, *49*, 1623–1626. (k) Rinehart, J. D.; Long, J. R. *Chem. Sci.* **2011**, *2*, 2078–2085.
- (8) Gonidec, M.; Biagi, R.; Corradini, V.; Moro, F.; Renzi, V. D.; del Pennino, U.; Summa, D.; Muccioli, L.; Zannoni, C.; Amabilino, D. B.; Veciana, J. *J. Am. Chem. Soc.* **2011**, *133*, 6603–6612.
- (9) (a) Rinehart, J. D.; Fang, M.; Evans, W. J.; Long, J. R. *J. Am. Chem. Soc.* **2011**, *133*, 14236–14239. (b) Rinehart, J. D.; Fang, M.; Evans, W. J.; Long, J. R. *Nat. Chem.* **2011**, *3*, 538–542.
- (10) (a) Benelli, C.; Gatteschi, D. *Chem. Rev.* **2002**, *102*, 2369–2387. (b) Osa, S.; Kido, T.; Matsumoto, N.; Re, N.; Pochaba, A.; Mrozinski, J. *J. Am. Chem. Soc.* **2004**, *126*, 420–421. (c) Sessoli, R.; Powell, A. K. *Coord. Chem. Rev.* **2009**, *253*, 2328–2341.
- (11) (a) Hussain, B.; Savard, D.; Burchell, T. J.; Wernsdorfer, W.; Murugesu, M. *Chem. Commun.* **2009**, 1100–1102. (b) Hewitt, I. J.; Lan, Y.; Anson, C. E.; Luzon, J.; Sessoli, R.; Powell, A. K. *Chem. Commun.* **2009**, 6765–6767. (c) Long, J.; Habib, F.; Lin, P.-H.; Korobkov, I.; Enright, G.; Ungur, L.; Wernsdorfer, W.; Chibotaru, L. F.; Murugesu, M. *J. Am. Chem. Soc.* **2011**, *133*, 5319–5328. (d) Chen, P.; Chen, H.; Yan, P.; Wang, Y.; Li, G. *CrystEngComm* **2011**, *13*, 6237–6242. (e) Guo, Y.-N.; Xu, G.-F.; Guo, Y.; Tang, J. *Dalton Trans.* **2011**, *40*, 9953–9963. (f) Ke, H.; Zhao, L.; Guo, Y.; Tang, J. *Eur. J. Inorg. Chem.* **2011**, 4153–4156. (g) Tian, H.; Guo, Y.-N.; Zhao, L.; Tang, J.; Liu, Z. *Inorg. Chem.* **2011**, *50*, 8688–8690. (h) Lin, S.-Y.; Wernsdorfer, W.; Ungur, L.; Powell, A. K.; Guo, Y.-N.; Tang, J.; Zhao, L.; Chibotaru, L. F.; Zhang, H.-J. *Angew. Chem., Int. Ed.* **2012**, *51*, 12767–12771. (i) Xue, S.; Zhao, L.; Guo, Y.-N.; Zhang, P.; Tang, J. *Chem. Commun.* **2012**, 48, 8946–8948. (j) Tian, H.; Wang, M.; Zhao, L.; Guo, Y.-N.; Guo, Y.; Tang, J.; Liu, Z. *Chem.—Eur. J.* **2012**, *18*, 442–445. (k) Anwar, M. U.; Tandon, S. S.; Dawe, L. N.; Habib, F.; Murugesu, M.; Thompson, L. K. *Inorg. Chem.* **2012**, *51*, 1028–1034. (l) Habib, F.; Long, J.; Lin, P.-H.; Korobkov, I.; Ungur, L.; Wernsdorfer, W.; Chibotaru, L. F.; Murugesu, M. *Chem. Sci.* **2012**, *3*, 2158–2164. (m) Mukherjee, S.; Chaudhari, A. K.; Xue, S.; Tang, J.; Ghosh, S. K. *Inorg. Chem. Commun.* **2013**, *35*, 144–148.

- (12) (a) Miao, Y.-L.; Liu, J.-L.; Li, J.-Y.; Leng, J.-D.; Oua, Y.-C.; Tong, M.-L. *Dalton Trans.* **2011**, 40, 10229–10236. (b) Sakaue, S.; Fuyuhiko, A.; Fukuda, T.; Ishikawa, N. *Chem. Commun.* **2012**, 48, 5337–5339. (c) Mei, X.-L.; Liu, R.-N.; Wang, C.; Yang, P.-P.; Li, L.-C.; Liao, D.-Z. *Dalton Trans.* **2012**, 41, 2904–2909.
- (13) Habib, F.; Brunet, G.; Vieru, V.; Korobkov, I.; Chibotaru, L. F.; Murugesu, M. *J. Am. Chem. Soc.* **2013**, 135, 13242–13245.
- (14) *SAINT Plus*, Version 7.03; Bruker AXS Inc.: Madison, WI, 2004.
- (15) Sheldrick, G. M. *SHELXTL, Reference Manual: Version 5.1*; Bruker AXS: Madison, WI, 1997.
- (16) Sheldrick, G. M. *Acta Crystallogr., Sect. A* **2008**, 112.
- (17) Farrugia, L. J. *WINGX, Version 1.80.05*; University of Glasgow: Glasgow, Scotland, 2011.
- (18) Spek, A. L. *PLATON, A Multipurpose Crystallographic Tool*; Utrecht University: Utrecht, The Netherlands, 2005.
- (19) (a) Langley, S. K.; Boujemaa, M.; Forsyth, C. M.; Gass, I. A.; Murray, K. S. *Dalton Trans.* **2010**, 39, 1705–1708. (b) Ungur, L.; Langley, S. K.; Hooper, T. N.; Moubaraki, B.; Brechin, E. K.; Murray, K. S.; Chibotaru, L. F. *J. Am. Chem. Soc.* **2012**, 134, 18554–18557.
- (20) (a) Zou, L.; Zhao, L.; Chen, P.; Guo, Y.-N.; Guo, Y.; Li, Y.-H.; Tang, J. *Dalton Trans.* **2012**, 41, 2966–2971. (b) Zhang, P.; Zhang, L.; Lin, S.-Y.; Xue, S.; Tang, J. *Inorg. Chem.* **2013**, 52, 4587–4592.
- (21) Tang, J.; Hewitt, I.; Madhu, N. T.; Chastanet, G.; Wernsdorfer, W.; Anson, C. E.; Benelli, C.; Sessoli, R.; Powell, A. K. *Angew. Chem., Int. Ed.* **2006**, 45, 1729–1733.
- (22) (a) Xue, S.; Zhao, L.; Guo, Y.-N.; Tang, J. *Dalton Trans.* **2012**, 41, 351–353. (b) Bernot, K.; Luzon, J.; Bogani, L.; Etienne, M.; Sangregorio, C.; Shanmugam, M.; Caneschi, A.; Sessoli, R.; Gatteschi, D. *J. Am. Chem. Soc.* **2009**, 131, 5573–5579.
- (23) (a) Guo, Y.-N.; Chen, X.-H.; Xue, S.; Tang, J. *Inorg. Chem.* **2011**, 50, 9705–9713. (b) Suzuki, K.; Sato, R.; Mizuno, N. *Chem. Sci.* **2013**, 4, 596–600.
- (24) (a) Blagg, R. J.; Ungur, L.; Tuna, F.; Speak, J.; Comar, P.; Collison, D.; Wernsdorfer, W.; McInnes, E. J. L.; Chibotaru, L. F.; Winpenny, R. E. P. *Nat. Chem.* **2013**, 5, 673–678. (b) Blagg, R. J.; Murny, C. A.; McInnes, E. J. L.; Tuna, F.; Winpenny, R. E. P. *Angew. Chem., Int. Ed.* **2011**, 50, 6530–6533.